Complex Planetary Systems II: Latest Methods for an Interdisciplinary Approach
Proceedings IAU Symposium No. 382, 2024
A. Lemaitre & A.-S. Libert, eds.
doi:10.1017/S1743921323004398

The obliquity of Mercury: Models and interpretation

Rose-Marie Baland

Royal Observatory of Belgium
email: rose-marie.baland@oma.be

Abstract. Mercury is locked in an unusual 3:2 spin-orbit resonance and as such is expected to be in a state of equilibrium called Cassini state. In that state, the angle between the spin axis and orbit normal, called obliquity, remains almost constant while the spin axis remains almost in the plane, also called Cassini plane, defined by the normal to the Laplace plane and the normal to the orbital plane. The spin axis and the orbit normal precess together with a period of about 300 kyr. The orientation of the spin axis of Mercury has been estimated using different approaches: (i) Earth-based radar observations, (ii) Messenger images and altimeter data, and (iii) Messenger radio tracking data. The different estimates all tend to confirm that Mercury occupies the Cassini state. The observed obliquity is small and close to 2 arcmin. It indicates a normalized polar moment of inertia of about 0.34. This information, combined with the existence of a liquid iron core, as evidenced by the librations, allows to constrain the interior structure of Mercury. However, the different estimates of the orientation of the spin axis locate the spin axis somewhat behind or ahead of the Cassini plane, and it is difficult to reconcile and interpret them coherently in terms of detailed interior properties. We review recent models for the obliquity and spin orientation of Mercury, which include the effects of complex orbital dynamics, tidal deformations and associated dissipation, and internal couplings related to the presence of fluid and solid cores. We discuss some implications regarding the interpretations of the orientation estimates in term of interior properties.

Keywords. planets and satellites: individual (Mercury), celestial mechanics, methods: analytical, obliquity, librations, geodesy, dynamics, rotation, planetary interiors

1. Introduction

1.1. *An unusual rotation*

Three important letters concerning the rotation of Mercury were published in 1965. First, using radar observations obtained at the Arecibo Ionospheric Observatory in Puerto Rico, Pettengill and Dyce (1965) determined that the rotation of Mercury is direct with a sidereal period of 59 ± 5 days which differs from the orbital period (88 days). They could not determine the direction of the pole, which is approximately normal to the planetary orbit. The fact that Mercury's rotation is not synchronous with its revolution was an unexpected discovery. Secondly, Peale and Gold (1965) noted that while for a planet in a circular orbit, tidal friction should synchronise its rotation with its revolution, the large eccentricity of Mercury (0.206) allows faster rotation because the tidal torque at pericenter, where the orbital angular velocity is maximum, exceeds that at other times. Finally, Colombo (1965) indicated that a uniform rotation with a period of 2/3 of the orbital period can be a stable state of rotation, because the axis of minimum moment of inertia (the largest axis in terms of dimension) is aligned with the Sun-Mercury direction at each pericenter passage, where the interaction between the two bodies is the strongest.

Table 1. Values of the orientation parameters of Mercury, obtained from different observational techiques. Based on Baland *et al.* (2017a) and Bertone *et al.* (2021).

Reference	Technique	$\alpha_0(^\circ)$	$\delta_0(^\circ)$
Margot *et al.* (2007)	Earth-based radar observations	281.0097	61.4143
Margot *et al.* (2012)	Earth-based radar observations	281.0103 ± 0.0015	61.4155 ± 0.0013
Mazarico *et al.* (2014)	MESSENGER radio tracking data	281.00480 ± 0.0054	61.41436 ± 0.0021
Stark *et al.* (2015)	Images and laser altimeter data from MESSENGER	281.00980 ± 0.00088	61.4156 ± 0.0016
Verma and Margot (2016)	MESSENGER radio tracking data	281.00975 ± 0.0048	61.41828 ± 0.0028
Genova *et al.* (2019)	MESSENGER radio tracking data	281.0082 ± 0.0009	61.4164 ± 0.0003
Konopliv *et al.* (2020)	MESSENGER radio tracking data	281.0138 ± 0.0025	61.4161 ± 0.0017
Bertone *et al.* (2021)	Images and laser altimeter data from MESSENGER	281.0093 ± 0.00063	61.4153 ± 0.00048

This part of the history of the study of Mercury's rotation is nicely documented in Sections 2 and 4 of Goldreich and Peale (1968).

1.2. *Cassini state*

Because the rotation rate of Mercury is commensurate with its orbital mean motion, the planet is assumed to be locked in a *Cassini state* and to follow Cassini's second and third laws (Peale 1969). In this state, the spin axis and the orbit normal precess together about the normal to the Laplace plane at the same rate (period of ~ 300 kyr), which means that all three axes are coplanar and the obliquity (the angle from the orbit normal to the spin axis) remains constant over time. The Laplace plane is the inertial plane that minimizes the variation in orbital inclination. In what follows, this particular state is referred to as the *Classical Cassini state*, as opposed to the more recent and advanced models which indicate that the spin axis can deviate by of a few arcsec from the Cassini plane (the plane defined by the Laplace and orbit normal axes), see Section 3.

2. Orientation measurements

2.1. *Published studies*

Using three different observational techniques, the orientation of Mercury's spin axis has been estimated no less than eight times since 2007, see Table 1. Each measurement is provided in terms of right ascension α_0 and declination δ_0 with respect to the International Celestial Reference Frame (ICRF) at the J2000 epoch, the format used by the IAU Working Group on Cartographic Coordinates and Rotational Elements of the Planets and Satellites. Almost all estimates listed in Table 1 are compatible with coplanarity/occupancy of the Classical Cassini state within the limits of measurements precision (see Fig. 1). The epoch spin location of Margot *et al.* (2012) is currently adopted by the IAU (Archinal *et al.* 2018). To those readers who desire more details on the evolution of the IAU adopted values for the rotation angles of Mercury, we recommend the articles by Margot (2009) and Stark *et al.* (2018).

2.2. *Obliquity/deviation representation*

Each pair (α, δ) corresponds to a pair of obliquity and deviation $(\varepsilon, \tilde{\delta})$, see Section 4.3 of Baland *et al.* (2017a) for the mathematical relationships. For example, the orientation of Stark *et al.* (2015) corresponds to an obliquity of about 2 arcmin and a deviation of 1.7 arcsec.

The obliquity/deviation representation is used in theoretical models to relate the estimated orientation to the interior properties of the planet, see Section 3. In particular,

https://doi.org/10.1017/S1743921323004398 Published online by Cambridge University Press

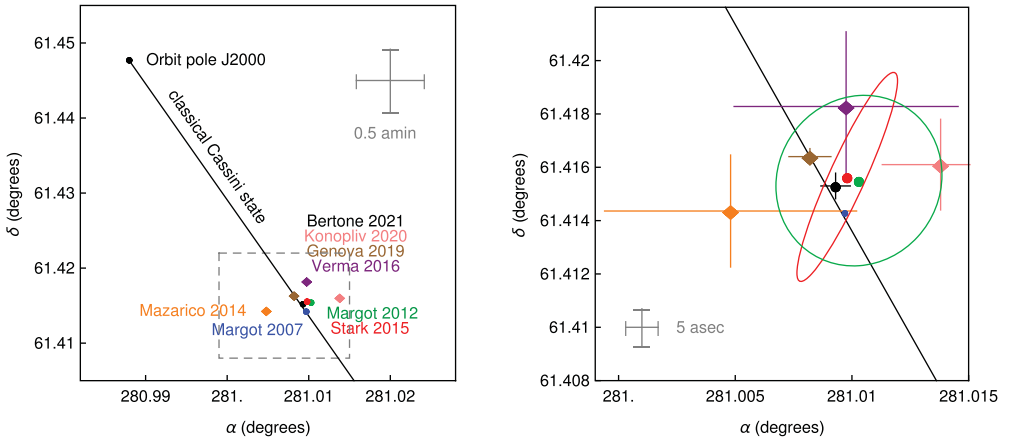

Figure 1. Orientation (right ascension α and declination δ w.r.t the ICRF) of the orbit pole and of the spin axis of Mercury at the J2000 epoch for the studies listed in Table 1. The solid line represents the location of the Cassini plane (Clasical Cassini state, see Section 1.2). The dashed rectangle on the left panel represents the plot limits used in the right panel (figure adapted from Baland *et al.* (2017a)).

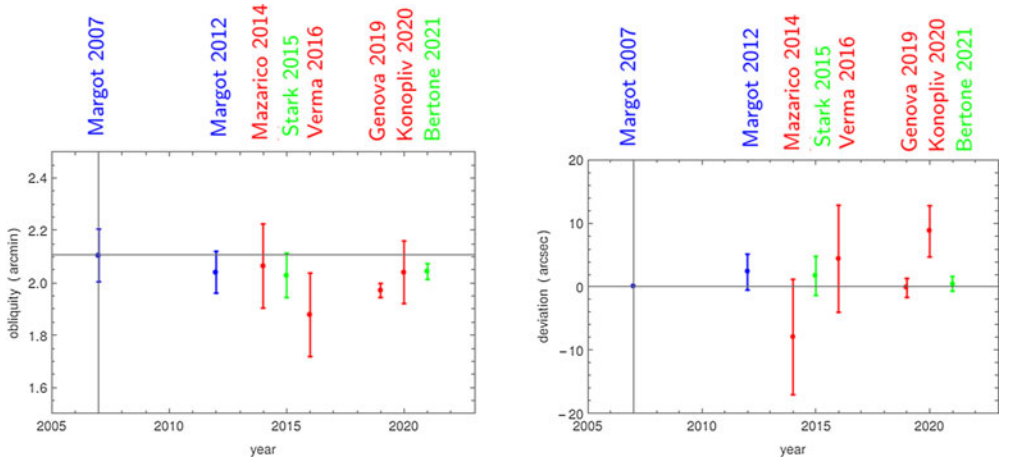

Figure 2. The different values for obliquity and deviation, according to the observational technique (Earth-based radar observations in blue - Messenger images and altimeter data in green - Messenger radio tracking data in red) and publication date.

the deviation $\tilde{\delta}$ represents the offest of the spin axis with respect to the Cassini plane and is zero in the Classical Cassini state.

From Margot *et al.* (2007) to Bertone *et al.* (2021), the estimated value for the obliquity has followed a downward trend (Fig. 2, left panel). As we will see in Section 3.2, this result has implication in terms of interior interpretation, and in particular in terms of the presence of a solid inner core. The estimated deviation started close to 0 with Margot *et al.* (2007). With the exception of Mazarico *et al.* (2014) and their negative deviation, $\tilde{\delta}$ is either close to 0, or follows an upward trend in subsequent studies (Fig. 2, right panel).

In some respects, the situation is reminiscent of the process of the determination of the elementary charge. Millikan's 1909 oil drop experiment, the initial direct determination of the magnitude of the elementary charge, yielded a value that we currently know slightly

https://doi.org/10.1017/S1743921323004398 Published online by Cambridge University Press

inaccurate due to his use of an incorrect value for the viscosity of the air. Although Millikan's first estimate was not correct, subsequent experimental attempts tended to be close to Millikan's, until they finally stabilized at a higher, correct value. To quote Feynman (1985): *"It's apparent that people did things like this: When they got a number that was too high above Millikan's, they thought something must be wrong and they would look for and find a reason why something might be wrong. When they got a number close to Millikan's value they didn't look so hard."* Were successive spin-axis orientation estimates influenced by the first obliquity estimate of Margot *et al.* (2007) and/or the authors' preconceived ideas about deviation? Since the discovery of the 3:2 spin orbit resonance of Mercury, the planet is reasonably considered to be in the Cassini state. Naturally, some authors did not imagine that the deviation could differ from zero, as appears clearly in Margot *et al.* (2007) † and Genova *et al.* (2019)‡. The possibility of a non zero deviation, and the implications in terms of energy dissipation due to solid-body tides and core-mantle interactions, was first recognized in Margot *et al.* (2012).

The authors sometimes explain the dispersion of their results by the different observation techniques used. On the one side, both the Earth-based radar (Margot *et al.* 2007, 2012) and laser altimeter (Stark *et al.* 2015; Bertone *et al.* 2021) determinations are specifically tied to the rotation of the solid surface layer, since Mercury has an at least partially liquid core. And indeed, all four orientation determinations (especially the last three) are in very good agreement with each other. They are characterized by similar obliquities despite differences in observational techniques. Despite a possible bias towards 0 at the beginning, they ultimately tend to indicate a small deviation. On the other side, the radio tracking determinations of Mazarico *et al.* (2014); Verma and Margot (2016); Genova *et al.* (2019); Konopliv *et al.* (2020) are allegedly tied to the orientation of the gravity field of the planet, and so we might expect to see them grouped together in Fig. 1. However, they are more scattered than the determinations tied to the surface, and marginally consistent with each other. Verma and Margot (2016) invoke the use of different ephemerides and range data to explain the difference between their estimate and that of Mazarico *et al.* (2014). The subsequent determinations of Genova *et al.* (2019) and Konopliv *et al.* (2020) did not resolved the differences. Topping it all off, the deviation is either negative, or positive but compatible with 0, or almost 0, or positive and not compatible with zero within the $1-\sigma$ limit.

3. Orientation modeling and interior interpretation

3.1. *Classical model*

The Classical Cassini state model for an entirely rigid Mercury comes with a relationship between the small obliquity ε and the polar moment of inertia C (see Eq. (4) of Peale 1981 and Eq. (12) of Yseboodt and Margot 2006):

$$\varepsilon = \frac{-C\dot{\Omega}\sin i}{C\dot{\Omega}\cos i + 2nM_{\mathrm{☿}}R^2G_{201}(e)C_{22} - nM_{\mathrm{☿}}R^2G_{210}(e)C_{20}} \tag{1}$$

† In Margot *et al.* (2007): *"The confidence regions for the spin orientation fall precisely on the locus of pole positions that satisfy the Cassini condition."* The Cassini condition referred to here is in fact the Classical Cassini state, with no deviation.

‡ Genova *et al.* (2019) argue that the spin pole orientations of Margot *et al.* (2012) and Stark *et al.* (2015) showed a *"substantial"* offset from the Cassini state, but that in contrast, their own estimate is in *"full agreement with the Cassini state"*, and by that, they mean the Classical Cassini state with a zero deviation.

https://doi.org/10.1017/S1743921323004398 Published online by Cambridge University Press

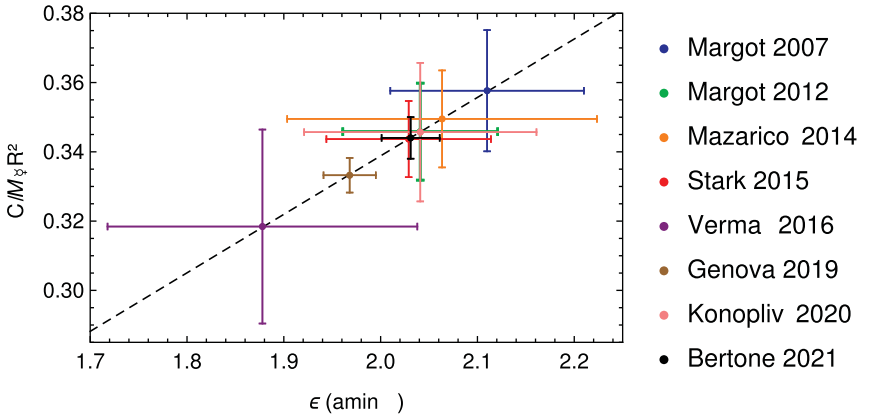

Figure 3. Normalized polar moment of inertia $C/M_{☿}R^2$ as a function of the obliquity ε. The solid line shows the quasi linear relationship resulting from Eq. (1) for the Classical Cassini state model.

where

$$G_{210}(e) = \left(1 - e^2\right)^{-3/2} \tag{2}$$

$$G_{201}(e) = \frac{7}{2}e - \frac{123}{16}e^3 + \frac{489}{128}e^5 + \mathcal{O}(e^7) \tag{3}$$

are eccentricity (e) functions, n is the mean motion, Ω and i are the longitude of the ascending node and orbital inclination with respect to the Laplace plane, $M_{☿}$ and R are the mass and mean radius of Mercury, and C_{20} and C_{22} are second-degree gravity field coefficients. Note that Eq. (1) has been derived independently in Baland *et al.* (2017a) to clarify the situation in the litterature, where uncorrect versions of the equation were in used, due to confusion regarding sign conventions (here the obliquity angle $\varepsilon > 0$ and the precession rate $\dot{\Omega} < 0$). Eq. (1) is obtained by assuming that Mercury behaves rigidly and that coplanarity is satisfied, so that no deviation is associated with the classical model.

Each estimate of the obliquity ($1.88 - 2.11$ arcmin) corresponds to an estimate of the normalized polar moment of inertia ($0.318 - 0.358$), see Fig. 3, which, together with the estimated mean density, indicates that Mercury is a differentiated body with a large iron core.

3.2. *Peale experiment*

To characterize the size and state of the core of Mercury, Peale (1976, 1981) proposed an observational procedure, since known as the *Peale experiment*. In the following equation

$$\left[\frac{(B-A)}{M_{☿}R^2}\right]\left[\frac{M_{☿}R^2}{C}\right]\left[\frac{C_m}{(B-A)}\right] = \frac{C_m}{C} \leq 1, \tag{4}$$

(i) the first factor is obtained from the second-degree and -order gravity coefficient C_{22}, (ii) the second factor is derived from the obliquity, using Eq. (1), and thus assuming that the core must follow the mantle on the time scale of forced precession, and (iii) the third factor is obtained from the forced libration at 88 days, the annual variation in the rotation due to the periodically reversing solar torque on the asymmetric figure, assuming that a liquid core would not follow the mantle's longitudinal oscillations. After multiplying these three factors, we obtain the ratio of the polar moment of inertia of the outer solid layer C_m over the total polar moment of inertia C. The ratio is 1 if the core is

https://doi.org/10.1017/S1743921323004398 Published online by Cambridge University Press

entirely solid, but is smaller if at least a part of the core is fluid. This procedure has been applied for example in Margot *et al.* (2007, 2012); Stark *et al.* (2015); Genova *et al.* (2019) and shows that $C_m/C \simeq 0.4$, indicating that the core is at least partially molten. The presence of a liquid core has important implications, as it provides a possible explanation based on a dynamo mechanism for the magnetic field observed by Mariner 10, helps to sort between thermal evolution models, and possibily explains the capture into resonance thanks to dissipation at the core-mantle boundary.

Considering a simple interior model consisting of two layers of uniform density, the ratio C_m/C implies that the size of the core ($\simeq 2000$ km) is $\simeq 80\%$ of the total radius and that the core and mantle densities are $\simeq 7250$ kg/m^3 and $\simeq 3200$ kg/m^3, respectively (Margot *et al.* 2012). Using more elaborate and realistic interior models and accurate estimates of the gravity coefficients by MESSENGER, Smith *et al.* (2012) or Hauck *et al.* (2013) estimated that the core radius is 2040 ± 37 or 2020 ± 30 km. Because their estimate of obliquity is lower than previous ones by Margot *et al.* (2007, 2012), Genova *et al.* (2019) derived a lower value for the polar moment of inertia and therefore concluded that Mercury has a solid inner core with a radius of at least 600 km (see also Steinbrügge *et al.* (2021)).

3.3. *Improving the experiment ?*

Annual libration

It has been shown that the relationship between the measured libration and the third factor of Eq. (4) is not valid (i) in the presence of a solid inner core, because of the gravitational-pressure coupling between the internal layers, and (ii) when the solid layers deform periodically. Tides decrease the forced annual libration amplitude, by about $1-2$ m, below the present and future expected observational precision, whereas an inner core larger than 1000 km could have a noticeable effect (Van Hoolst *et al.* 2012; Dumberry *et al.* 2013).

To avoid possible biases in the interpretation of rotation measurements in terms of interior structure, due to simplistic modeling of librations, Rivoldini and Van Hoolst (2013) has somewhat redesigned the *Peale experiment*. As the annual libration amplitude cannot be expressed as a function of the equatorial moment of inertia difference $(B-A)$ of the whole body (compare Eqs. 8 and 11 of Rivoldini and Van Hoolst (2013)), the improved experiment, unlike Eq. (4), can no longer be written in an elegant form to first obtain the moment of inertia of the silicate shell, which will then be interpreted in terms of interior properties. Instead, Rivoldini and Van Hoolst (2013) used as data the mean moment of inertia and the annual libration amplitude of Margot *et al.* (2012) in combination with the libration model of Van Hoolst *et al.* (2012) to directly constrain Mercury's interior structure.

Considering elaborate interior models that include a crust and an inner core, non uniform layers, and plausible chemical compositions and temperature profiles, see also Rivoldini *et al.* (2009) for additional details, they placed a lower constraint on the core radius (2004 ± 39 km) than Smith *et al.* (2012); Hauck *et al.* (2013), due to the mantle-core coupling taken into account in the libration model. They also determined the average density of the core (7233 ± 267 kg/m^3) and the fraction of sulfur in the core if sulfur is the only light element in the core ($4.5 \pm 1.8 wt\%$). They could not however confirm or infirm the existence of an inner core or impose constraints on the mantle density. According to Dumberry and Rivoldini (2015), which also use the rotation measurements of Margot *et al.* (2012), the largest inner core compatible with the rotation observations has a radius of 1325 ± 250 km, and geodetic observations suggest the formation of Fe-snow within the fluid core that could contribute to the magnetic field. The conclusions drawn

https://doi.org/10.1017/S1743921323004398 Published online by Cambridge University Press

by Rivoldini and Van Hoolst (2013); Dumberry and Rivoldini (2015) depend strongly on the chosen value of the polar moment of inertia, derived from the measured obliquity.

Obliquity

The relationship between obliquity and interior structure as provided by Eq. (1), and used to obtain the second factor of Eq. (4), needs to be questioned. Baland *et al.* (2017a) have listed various approximations in the modeling process that affect the determination of the polar moment of inertia from the measured orientation of the rotation axis. Among these, the most important are neglecting (i) the nutations due to the precession of the pericenter, (ii) the periodic tidal deformations, and (iii) the presence of a solid inner core (see details below). The use of an improved Cassini state model instead of Eq. (1) may, as with improved libration models, modify the interpretation of rotation measurements in terms of interior structure.

Using other observations

Finally, Peale's experiment can be extended to observations other than obliquity and annual libration, although in this case we can no longer really speak of Peale's experiment. For example, the long period libration (11.864 years) due to the orbital perturbations of Mercury's orbit by Jupiter could be resonantly amplified and affect the instantaneous spin rate, so that it deviates from the resonant rate (Stark *et al.* 2015, Yseboodt *et al.* 2013 and references within). In addition to rotation, the observed tidal Love numbers (see Mazarico *et al.* (2014); Verma and Margot (2016); Genova *et al.* (2019); Konopliv *et al.* (2020) for k_2 and Bertone *et al.* (2021) for h_2) and deviation of the spin axis from coplanarity (see below) can also contribute to a detailed study of Mercury's interior structure and rheology (e.g. Rivoldini *et al.* 2009; Padovan *et al.* 2014; Margot *et al.* 2018; Steinbrügge *et al.* 2021; Goossens *et al.* 2022). Note that the measured k_2, larger than expected for an entirely solid Mercury, confirms the presence of a liquid core, whereas the measured h_2 suggests the presence of a solid inner core.

3.4. *Cassini state: Effect of pericenter precession*

According to Baland *et al.* (2017a), assuming that Mercury rotates as a solid rigid body on very long timescales, the angular momentum equation governing the motion of its spin axis in space can be written in an inertial reference frame attached to the Laplace plane and centered at the center of mass of the planet as

$$\frac{d\vec{L}}{dt} = \vec{\Gamma}^{prec} + \vec{\Gamma}^{nut} \tag{5}$$

with $\vec{L}$ the angular momentum and $\vec{\Gamma}^{prec}$ and $\vec{\Gamma}^{nut}$ the two parts of the torque exerted by the Sun on Mercury. The solution for $\vec{L}$ is associated to time-varying obliquity and deviation:

$$\varepsilon(t) \simeq \varepsilon_\Omega + \varepsilon_\omega \cos 2\omega(t), \tag{6}$$

$$\tilde{\delta}(t) \simeq \varepsilon_\omega \sin 2\omega(t). \tag{7}$$

The main torque $\vec{\Gamma}^{prec}$ is caused by the precession of the orbital node (Ω, with a period of $\sim 325\,000$ years) and, alone, leads to a spin precession characterized by a constant obliquity ε_Ω given by Eq. (1) and a zero deviation. The classically neglected secondary part $\vec{\Gamma}^{nut}$ is caused by the precession of the orbital pericenter (ω, period of $\sim 134\,000$ years) and the large eccentricity e, and drives a small and very slow nutation about the

https://doi.org/10.1017/S1743921323004398 Published online by Cambridge University Press

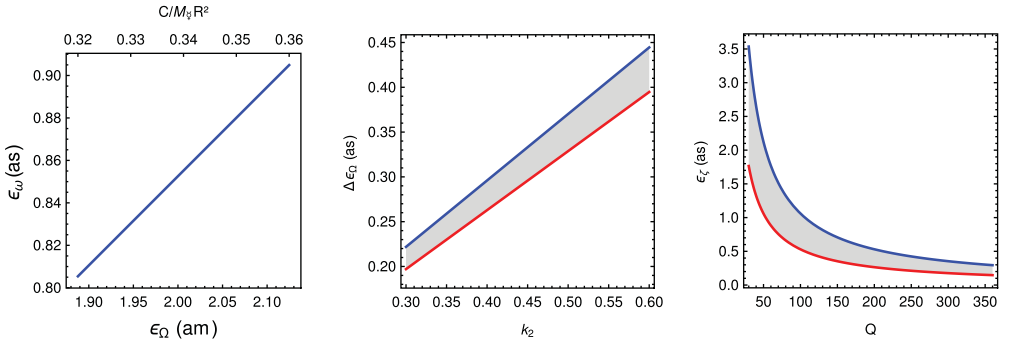

Figure 4. From left to right: nutation amplitude ε_ω as a function of the precession amplitude ε_Ω, tidal shift in obliquity $\Delta\varepsilon_\Omega$ as a function of k_2 ($C/M_m R^2 = 0.32$ and 0.36 for the bottom and top curves, respectively), and tidal shift in deviation as a function of Q ($k_2 = 0.3$ and 0.6 for the bottom and top curves, respectively), taken from Baland *et al.* (2017a).

main precession with the amplitude ε_ω, leading to periodic variations in obliquity and deviation with respect to the coplanarity. Due to the nutation, coplanarity is therefore very unlikely.

The amplitude ε_ω of the nutation is proportional to the amplitude ε_Ω of the main precession. For $C/M_{\mathrm{☿}}R^2$ ranging from 0.32 to 0.36, ε_ω ranges between 0.8 and 1 arcsec, see Fig. 4 (left panel). Since $\omega(0) = 50.379554°$, $\varepsilon(0)$ is reduced by 0.15 to 0.19 arcsec ($\sim 0.14\%$) with respect to ε_Ω and the deviation $\tilde{\delta}(0)$ is positive and ranges between 0.8 and 1 arcsec.

The nutation induced by the pericenter precession is essential to explain and interpret any observed positive deviation. The deviation related to the nutation is about half the observed deviation of Stark *et al.* (2015) for instance. The nutation results from the orbital dynamics and certainly does exist, even though it was classically neglected. In Peale (1974), the Hamiltonian includes one term that would lead to nutation induced by the pericenter precession, if it had not been neglected on the grounds that it is of third order in eccentricity. Peale *et al.* (2016) numerically identifies the nutation in their model.

3.5. *Cassini state: Effet of solid tides and associated dissipation*

Even assuming that Mercury rotates as a solid body on very long timescales, it deforms tidally at the orbital period, which consequently modifies the solar torque through (i) the tidal Love number k_2, which describes changes in the external gravitational potential, and (ii) the quality factor Q associated with tidal dissipation and corresponding to a phase shift $\zeta = 1/Q$ in the mean anomaly in the torque expression. Due to solid tides, the angular momentum of Mercury is affected by a constant shift in orientation over time. The solution for the time-varying obliquity and deviation, including both the nutation due to the pericenter precession and the constant shift in orientation due to the solid tides reads, see Baland *et al.* (2017a):

$$\varepsilon(t) \simeq \varepsilon_\Omega + \Delta\varepsilon_\Omega + \varepsilon_\omega \cos 2\omega(t), \tag{8}$$

$$\tilde{\delta}(t) \simeq \varepsilon_\zeta + \varepsilon_\omega \sin 2\omega(t). \tag{9}$$

The estimated k_2 of Mercury varies between 0.45 and 0.57 (see Mazarico *et al.* (2014); Verma and Margot (2016); Genova *et al.* (2019); Konopliv *et al.* (2020), whereas Q, as yet unestimated, probably lies in the interval $[30, 360]$ that covers current estimates for the Earth, the Moon and Mars (Lainey 2016). The shift in obliquity $\Delta\varepsilon_\Omega$ is proportional to k_2, positive, and varies from ~ 0.30 to ~ 0.45 arcsec ($\sim 0.30\%$) for k_2 in the interval

https://doi.org/10.1017/S1743921323004398 Published online by Cambridge University Press

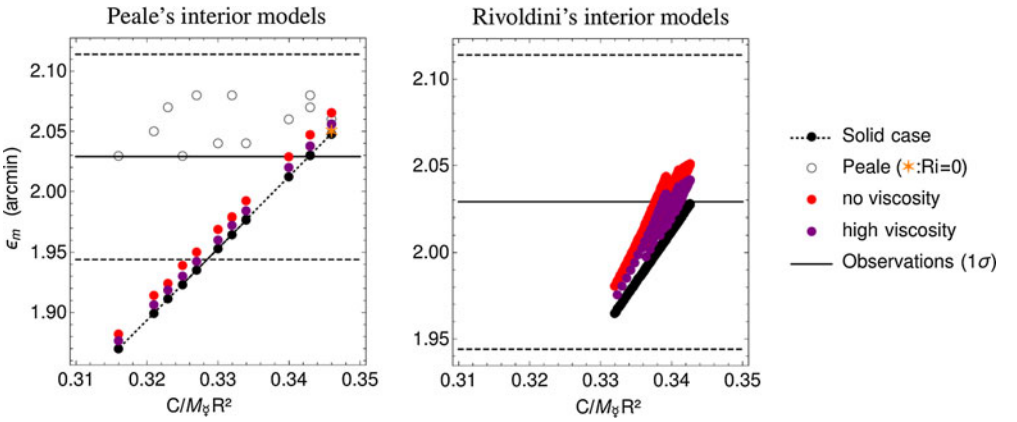

Figure 5. Mantle obliquity of Mercury as a function of the normalized polar moment of inertia for the set of 13 interiors structure models defined in Peale *et al.* (2016) (left panel) and for a large set of realistic interior models consistent with the annual libration amplitude and based on Rivoldini and Van Hoolst (2013). The black dots indicate the solid case obliquities according to Eq. (1), the clear dots represent the results of Peale *et al.* (2016) (their Table 1), the purple and red dots represent the results of Baland *et al.* (2017b), and the solid and dashed line represent the measured obliquity of Margot *et al.* (2012). Note that the radius of the inner core R_i increases with decreasing MOI and that one of Peales's interior model, with $R_i = 0$, has no solid inner core and the largest MOI. Figure adapted from from Baland *et al.* (2017b).

$[0.45, 0.60]$, see Fig. 4 (middle panel). The shift in deviation ε_ζ is inversely proportional to Q, positive, and of the order of 1 arcsec (Fig. 4, right panel).

Note that the tidal Love number k_2 cannot be inferred from an obliquity measurement, because it appears in $\Delta\varepsilon_\Omega$ and would be correlated with the polar moment if inertia which appears in ε_Ω. This is why it is useful to analyze tidal and rotational measurements together. The shift in deviation due to solid body tides, also identified analytically in MacPherson and Dumberry (2022), along with the deviation associated with pericenter precession-induced nutation, could explain any observed positive deviation of a few arcsec and help to constrain Mercury's interior structure and rheology.

3.6. *Cassini state: Effect of the fluid outer core and the inner core*

As shown by the measured annual librations and the tidal Love number k_2, the core of Mercury is at least partially molten. The presence of a solid inner core is suspected, although the conclusion seems to depend on the value considered for the polar moment of inertia: Genova *et al.* (2019), thanks to their small obliquity, claim to have confirmed its presence, while Rivoldini and Van Hoolst (2013) using the larger obliquity of Margot *et al.* (2012) were unable to settle the question. In the presence of a solid inner core, internal gravitational-pressure and magnetic-viscous couplings between the internal layers could significantly influence the obliquity of the planet, thus affecting its interpretation in terms of interior. However, contradictory results coexist on this subject in the literature.

Peale *et al.* (2016) computed the mantle obliquity ε_m for a limited set of 13 interior structure models, see Fig. 5 (left panel). For each interior model, ε_m is larger (up to $5-10\%$) than the solid case obliquity ε of Eq. (1). It should be noted that no clear relationship between ε_m and $C/M_{☿}R^2$ emerges from these results, which is intriguing. Baland *et al.* (2017b) tried to reproduce the results for the same set of interior models and found other values for ε_m, which depend linearly on $C/M_{☿}R^2$. They also found that the modeled obliquity ε_m is only 0.5 to 1% larger than the solid case obliquity.

https://doi.org/10.1017/S1743921323004398 Published online by Cambridge University Press

Dumberry (2021), for a different set of interior models which satisfy exactly the value of $C/M_{\mathrm{☿}}R^2 = 0.3455$, concluded that the presence of a solid inner core affects the mantle obliquity by as much as 0.5%.

The problem with the results discussed above is that they are based on a set of interior models that is unrepresentative of the current knowledge of Mercury's internal structure. Baland *et al.* (2017b), using a set of plausible interior structure models based on Rivoldini and Van Hoolst (2013), found that the modeled obliquity may be up to 2% larger than the solid case obliquity, see Fig. 5 (right panel). An additional increase in mantle obliquity arises in the presence of a solid inner core, due to the elastic deformations caused by the misalignment of the solid layers, which perturb the obliquity as much as the tidal deformations due to gravitational potential of the Sun (MacPherson and Dumberry 2022).

All in all, interpreting a measured obliquity with a model which includes the effect of pericenter precession, solid body tides, and the internal couplings between the internal layers, instead of the Classical Cassini state model, may lead to a polar moment of inertia decreased by up to $\sim 2\%$ and therefore to a more differentiated interior more likely to include a solid inner core. For now, the actual precision $(3-4\%)$ on the orientation precludes further constraints on Mercury's interior.

4. Conclusion

Mercury is in a 3:2 spin-orbit resonance and is most likely locked in a Cassini state, as different estimates of the orientation of its spin axis tend to confirm. Precise modeling of the rotation is required to interpret these measurements in terms of the planet's inner properties. The most advanced theoretical models predict a slightly larger obliquity than the classical Peale's equation, making the presence of a solid inner core slightly more likely. The advanced models also predict a deviation of a few arcsec from coplanarity, in agreement with most observations. On the basis of theoretical modelling, it is practically impossible for the actual deviation to be zero. Long-period librations, tidal Love numbers, and deviation of the spin axis can be used in combination with measured obliquity, annual libration, and gravity field and with advanced rotation models to constrain Mercury's interior structure and rheology more precisely than with Peale's experiment.

5. Acknowledgment

I am grateful to my colleagues on this topic: Marie Yseboodt, Attilio Rivoldini and Tim Van Hoolst. This work was financially supported by the Belgian PRODEX program managed by the European Space Agency in collaboration with the Belgian Federal Science Policy Office.

References

Archinal, B. A. and A'Hearn, M. F. and Bowell, E., *et al.* 2011, *Celestial Mechanics and Dynamical Astronomy*, 109, 101–135

B.A. Archinal, C.H. Acton, M. F. A'Hearn, *et al.* 2018, *Celestial Mechanics and Dynamical Astronomy*, 130, 22

Baland, R.-M., Yseboodt, M., Rivoldini, A., *et al.* 2017a, *Icarus*, 291, 136–159

Baland, R.-M., Yseboodt, M., Rivoldini, A., *et al.* 2017b, *European Planetary Science Congress*, EPSC2017–521

Bertone, S., Mazarico, E., Barker, M. K., *et al.* 2021, *Journal of Geophysical Research (Planets)*, 126, e06683

Colombo, G. 1965, *Nature*, 208, 575

Dumberry, M., Rivoldini, A., Van Hoolst, T., Yseboodt, M. 2013, *Icarus*, 225, 62–74

Dumberry, M., Rivoldini, A., 2015, *Icarus*, 248, 254–268

Dumberry, M. 2021, *Journal of Geophysical Research (Planets)*, 126, e06621
Feynman, Richard P. 1985, Surely you're joking Mr. Feynman!, New York: W.W.Norton
Genova, A., Goossens, S., Mazarico, E., *et al.* 2019, *Geophysical Research Letters*, 46, 3625–3633
Goldreich, Peter and Peale, Stanton J. 1968, *Annual Review of Astronomy and Astrophysics*, 6, 287
Goossens, S., Renaud, J. P., Henning, W. G., *et al.* 2022, *The Planetary Science Journal*, 3, 37
Hauck, S. A., Margot, J.-L., Solomon, S. C., *et al.* 2013, *Journal of Geophysical Research (Planets)*, 118, 1204–1220
Konopliv, A. S., Park, R. S., Ermakov, A. I. 2020, *Icarus*, 335, 113386
Lainey, V. 2016, *Celestial Mechanics and Dynamical Astronomy*, 126, 145–156
MacPherson, I., Dumberry, M. 2022, *Journal of Geophysical Research (Planets)*, 127, e07184
Margot, J. L., Peale, S. J., Jurgens, R. F., *et al.* 2007, *Science*, 316, 710–714
Margot, J. L. 2009, *Celestial Mechanics and Dynamical Astronomy*, 105, 329–336
Margot, J. L., Peale, S. J., Solomon, S. C., *et al.* 2012, *Journal of Geophysical Research (Planets)*, 117, E00L09
Margot, J.-L., Hauck, S. A., Mazarico, E., *et al.* 2018, Mercury's Internal Structure, Mercury The View after MESSENGER: Cambridge University Press
Mazarico, E., Genova, A., Goossens, S., *et al.* 2014, *Journal of Geophysical Research (Planets)*, 119, 2417–2436
Padovan, S., Margot, J.-L., Hauck, S. A., *et al.* 2014, *Journal of Geophysical Research (Planets)*, 119, 850–866
Peale, S. J. and Gold, T. 1965, *Nature*, 206, 1240–1241
Peale, S. J. 1969, *Astronomical Journal*, 74, 483–489
Peale, S. J. 1974, *Astronomical Journal*, 79, 722
Peale, S. J. 1976, *Nature*, 262, 765–766
Peale, S. J. 1981, *Icarus*, 48, 143–145
Peale, S. J, Margot, J.-L., Hauck, S. A., Solomon, S. C. 2016, *Icarus*, 264, 443–455
Pettengill, G. H. and Dyce, R. B. 1965, *Nature*, 206, 1240
Rivoldini, A., Van Hoolst, T., Verhoeven, O. 2009, *Icarus*, 201, 12–30
Rivoldini, A., Van Hoolst, T. 2013, *Earth and Planetary Science Letters*, 377, 62–72
Smith, D. E., Zuber, M. T., Phillips, R. J., *et al.* 2012, *Science*, 336, 214
Stark, A., Oberst, J., Preusker, F., *et al.* 2015, *Science*, 117, 64–72
Stark, A., Oberst, J., Preusker, F., *et al.* 2018, *Journal of Geodesy*, 92, 949–961
Steinbrügge, G., Dumberry, M., Rivoldini, A., *et al.* 2021, *Geophysical Research Letters*, 48, e89895
Van Hoolst, T., Rivoldini, A., Baland, R.-M., Yseboodt, M. 2012, *Earth and Planetary Science Letters*, 333, 83–90
Verma, A. K., Margot, J.-L. 2016, *Journal of Geophysical Research (Planets)*, 121, 1627–1640
Yseboodt, M., Margot, J.-L. 2006, *Icarus*, 181, 327–337
Yseboodt, M., Rivoldini, A., Van Hoolst, T., Dumberry, M. 2013, *Icarus*, 226, 41–51